

## Gravity currents propagating up a slope

Larissa J. Marleau,<sup>1,a)</sup> Morris R. Flynn,<sup>2,b)</sup> and Bruce R. Sutherland<sup>3,c)</sup>

<sup>1</sup>*Department of Mechanical Engineering, University of Alberta, Edmonton, Alberta T6G 2G8, Canada*

<sup>2</sup>*Department of Mechanical Engineering, University of Alberta, Edmonton, Alberta T6G 2E1, Canada*

<sup>3</sup>*Department of Physics and Earth and Atmospheric Sciences, University of Alberta, Edmonton, Alberta T6G 2E3, Canada*

(Received 15 January 2014; accepted 9 April 2014; published online 23 April 2014)

Bottom propagating gravity currents resulting from full- and partial-depth lock-release experiments are investigated as they approach and then propagate up a rising slope. Consistent with the prediction of a WKB-like theory, the gravity current front decelerates in a nearly uniform manner along the slope as  $0.112g's(D/H)(2 - D/H)$ , in which  $g'$  is the reduced gravity,  $s$  is the slope,  $D$  is the initial lock-fluid height, and  $H$  is the ambient fluid height. The shape of the gravity current as it decelerates over relatively steep slopes is found to be self similar with a nearly linear decrease of the head height between the start of the slope and up to 80% of the distance to the nose. Some deviation from self-similar behaviour is found in cases with small  $s$  because of the comparatively large volume of fluid in the gravity current tail that flows downslope while the front continues to advance upwards. © 2014 AIP Publishing LLC. [<http://dx.doi.org/10.1063/1.4872222>]

### I. INTRODUCTION

A gravity current is a primarily horizontal flow caused by a density difference between the current and the ambient fluid.<sup>1-3</sup> Gravity currents are manifest in nature as thunderstorm outflows, sea breezes, salt wedges in estuaries, etc. In industrial processes, they are manifest as part of chemical mixing, accidental gaseous releases, buoyancy-driven ventilation processes, etc.<sup>2</sup> Gravity currents have been well studied by way of theory, laboratory experiments, and numerical simulations for the special case in which they travel along a flat, horizontal surface<sup>4-12</sup> or over small obstacles.<sup>13</sup> Benjamin<sup>6</sup> modelled steady gravity currents using a reference frame that moved with the gravity current front. He required mass and the flow force to be conserved and thereby derived a formula for the speed of the gravity current as a function of the height of the gravity current, the height of the ambient fluid, and the density difference between the two fluids. Additionally, assuming energy conservation, he predicted the current should span half the ambient depth. Benjamin's<sup>6</sup> was a local analysis centred on the gravity current front, whereas other investigators considered the explicit influence of initial conditions. Rottman and Simpson<sup>9</sup> applied shallow water theory coupled to Benjamin's<sup>6</sup> front condition and they performed full-depth lock-release gravity current experiments to show that a current moved at constant speed until it had propagated six to ten lock-lengths. Thereafter, the flow began to decelerate and transitioned to the buoyancy-inertia self-similar phase.<sup>9,11,14</sup> Shin *et al.*<sup>10</sup> developed a theory that tested well against experimental measurements and which examined the speed of partial-depth lock-release gravity currents, presumed to be energy conserving.

<sup>a)</sup>Email: [lmarleau@ualberta.ca](mailto:lmarleau@ualberta.ca)

<sup>b)</sup>Author to whom correspondence should be addressed. Electronic mail: [mrfflynn@ualberta.ca](mailto:mrfflynn@ualberta.ca). URL: [web-srv.mece.ualberta.ca/mrfflynn](http://web-srv.mece.ualberta.ca/mrfflynn).

<sup>c)</sup>Email: [bruce.sutherland@ualberta.ca](mailto:bruce.sutherland@ualberta.ca). URL: [www.ualberta.ca/~bsuther](http://www.ualberta.ca/~bsuther).

There have been relatively few laboratory studies of gravity currents moving downslope.<sup>15–19</sup> Britter and Linden<sup>15</sup> showed that, even for small inclination angles, the current resulting from a constant volume flux source propagated at constant speed far downslope as a result of the balance between gravity, that accelerates the flow, and basal friction and entrainment, which have a retarding influence.

Regarding upslope flow, experiments are presently being conducted by Adduce and colleagues (personal communication) who are investigating bottom propagating gravity currents on up sloping beds with slopes ranging from 0 to 0.027 to assess the accuracy of numerical entrainment models. Their numerical code, which solves the two-layer shallow water equations, is an extension of that used in an earlier study<sup>20</sup> of horizontally propagating currents.

The purpose of this investigation is to examine the evolution of bottom propagating gravity currents from full- and partial-depth locks as they encounter a rising uniform slope ranging from moderately shallow to steep. Besides the fundamental interest in exploring how fast and how far the current moves upslope, this research more broadly constitutes the start of a theoretical and laboratory experimental program investigating the advance of sea breezes over complex coastal terrain in order to provide a better understanding of their impact upon vegetation, industry, and communities. An example of an agricultural application is the influence of sea breezes that bring moisture and cooler temperatures to the inland wineries near Santa Barbara, CA.

In Sec. II, existing theories for gravity currents in uniform-depth ambients are adapted using a WKB-type<sup>22</sup> analysis so as to predict how the front position changes in time when passing over a shallow slope. Section III describes the setup of the lock-release experiments. Also outlined are the image processing algorithms and analyses used to determine the horizontal velocity, deceleration profile, and time varying shape of the gravity currents. In Sec. IV, measurements of front position versus time are compared against the predictions of the WKB-like theory and the parameters that affect the shape of the gravity current during the deceleration phase are identified. Finally, Sec. V gives a summary of key results.

## II. THEORY

Within this investigation the speed,  $u$ , of an inviscid, steady-state gravity current propagating over a horizontal surface in an ambient fluid of depth  $H$ , is written in terms of a Froude number,  $Fr_H$ , by  $U = Fr_H \sqrt{g'H}$  in which  $g' \equiv g(\rho_\ell - \rho_a)/\rho_a$  is the reduced gravity based on the current and ambient densities,  $\rho_\ell$  and  $\rho_a$ , respectively. Benjamin's steady-state analysis<sup>6</sup> predicted  $Fr_H = [\delta(1 - \delta)(2 - \delta)/(1 + \delta)]^{1/2}$  in which  $\delta \equiv h/H$  is the ratio of the gravity current height,  $h$ , to  $H$ . Additionally, assuming energy conservation, Benjamin<sup>6</sup> predicted a current should occupy half the channel depth, i.e.,  $\delta = 1/2$  and so  $Fr_H = 1/2$ . This prediction was reasonably well borne out in full-depth lock-release experiments,<sup>10,21</sup> which found  $\delta \simeq 0.5$  and  $Fr_H \simeq 0.45$ . The minor discrepancy between theory and experiment indicated that the energy loss associated with mixing was a small fraction of the kinetic and available potential energies of the flow.<sup>10,12</sup> Benjamin<sup>6</sup> further predicted the speed of a steady gravity current in an infinitely deep ambient to be  $U = \sqrt{2g'h}$ . However, because his theory did not explicitly take into consideration the initial conditions, it was unable to give a deterministic prediction for the speed of partial-depth lock-release gravity currents.

By considering the return flow into the lock as well as the advancing gravity current head, Shin *et al.*<sup>10</sup> extended Benjamin's<sup>6</sup> analysis to predict the speed of energy-conserving gravity currents released from partial-depth locks. In particular, Shin *et al.*<sup>10</sup> predicted the current depth to be  $h = D/2$ , where  $D$  is the initial depth of the gravity current fluid inside the lock. By extension, they predicted the front speed to be

$$U = Fr_D \sqrt{g'H}, \quad (1)$$

where

$$Fr_D = \sqrt{\delta(1 - \delta)}. \quad (2)$$

Explicitly, in the full-depth lock-release limit,  $D \rightarrow H$  ( $\delta \rightarrow 1/2$ ), it can be seen that  $Fr_D \rightarrow 1/2$ , which equals  $Fr_H$  in the limit corresponding to an energy conserving half-depth gravity current.

The predictions for both  $h$  and  $U$  reduced to those of Benjamin<sup>6</sup> for full-depth lock-release currents ( $D = H$ ). However, in the limit  $D \ll H$ , they found  $U/\sqrt{g'h} = 1$  instead of  $\sqrt{2}$ . Though their theory involved the simplifying assumptions of energy conservation and negligible vertical accelerations, its predictions were in strong agreement with the results of laboratory experiments (e.g., see Figure 14 of Shin *et al.*<sup>10</sup>).

Both Benjamin<sup>6</sup> and Shin *et al.*<sup>10</sup> assumed that  $\text{Re} \gg 1$ , so that viscosity had a negligible effect on the average velocity of the gravity current. The same assumption is used in this investigation and holds true provided  $D/H$  is not very small. Viscosity is known to affect instabilities that develop along the current front and consequent mixing behind the head. Experiments have shown, however, that these instabilities exert little influence upon the mean spreading of the current head,<sup>23</sup> which in turn explains the success of two-dimensional numerical simulations in modelling the bulk features of the flow.

To predict how the current front slows down over the slope, a WKB-like approach is taken. This is similar to that used by Sutherland *et al.*,<sup>24</sup> who examined surface gravity currents shoaling over sloping topography. It is assumed that the front deceleration along the slope is caused only by the decreasing ambient fluid height. Consistent with studies of downslope gravity current flow, the influence of the along-slope component of gravity is assumed to be negligible compared to that of the return flow of the ambient above the current head. This is likely a poor assumption if  $D/H$  is sufficiently small. However, as we demonstrate in the experiments results that follow, it appears to be a quite good assumption for  $D/H \geq 1/2$ . The Froude number is assumed to be a constant,  $\text{Fr}_D = F_0$ , while the current propagates upslope into an ambient of decreasing height,  $H_s(x)$ , where  $x$  denotes the horizontal coordinate. This assumption is equivalent to the requirement that the ratio of the current height to the ambient depth remains constant throughout the upslope propagation (e.g., see Sec. 11.6.4 in Simpson<sup>2</sup>). Together with (1), in which  $U \equiv dx/dt$ , this gives

$$\frac{dx}{dt} = F_0 (g' H_s(x))^{1/2}. \quad (3)$$

For the case of a uniform slope,  $H_s(x) = H - sx$  for  $x > 0$ , the solution of (3) is

$$x(t) = -\frac{1}{4} F_0^2 g' s t^2 + U_0 t, \quad (4)$$

in which  $U_0$  is the speed of the incident current when it first encounters the slope at  $t = 0$ . Therefore, the current should undergo a constant deceleration whose horizontal component has magnitude  $d_x = F_0^2 g' s / 2$ . Using (2), this is given in terms of  $D$  and  $H$  by

$$d_x = \frac{1}{2} g' s \delta (1 - \delta) = \frac{1}{8} g' s \frac{D}{H} \left( 2 - \frac{D}{H} \right). \quad (5)$$

In particular, for full-depth lock-release currents ( $D/H = 1$ ),  $d_x = g' s / 8$ .

For any value of  $D/H$ , the maximum horizontal distance traversed by the gravity current as it runs upslope is

$$x_{\max} = \frac{U_0^2}{\delta(1-\delta)g's} = \frac{H}{s}, \quad (6)$$

in which the last expression is derived using (1). The corresponding maximum height measured from the tank bottom is  $z_{\max} = s x_{\max} = H$ . Of course if  $D/H$  is small, in which case the initial available potential energy of lock-fluid is also small, the front is not expected to rise up to the top of the slope. This serves as a reminder that the neglect of the along-slope component of  $g'$  in the derivation of (5) and (6) is reasonable only in the limit of sufficiently large  $D/H$ .

An alternate prediction for the deceleration that implicitly accounts for the effect of along-slope gravitational deceleration requires that the velocity of a gravity current must decrease as its kinetic energy is converted to potential energy. Heuristically one might expect the current to rise upslope a vertical distance  $D$ , equal to its initial height in the lock. Assuming the current undergoes a constant deceleration as it rises upslope and that it stops at a vertical height  $D$ , the horizontal deceleration is

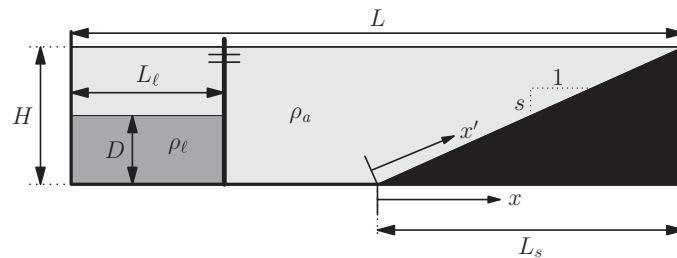


FIG. 1. Schematic side-view of the setup before the start of an experiment with salt water of density  $\rho_\ell$  and depth  $D$  (dark grey) located behind a gate in a lock of length  $L_\ell$ . A uniform slope of base length  $L_s$  and height  $H$  is situated to the right (shaded black beneath the slope).

predicted to be

$$d_x = \frac{U_0^2}{2(D/s)} = \frac{1}{8}g's \left(2 - \frac{D}{H}\right). \quad (7)$$

Predictions (5) and (7) will be tested through lab experiments.

### III. EXPERIMENT SETUP AND ANALYSIS

#### A. Tank setup

The setup for these experiments is illustrated in Figure 1. Experiments were performed in a long rectangular glass tank of interior length  $L = 197.5$  cm, width 17.6 cm, and total height 48.5 cm. In all cases, the tank was filled with fresh water to a height of  $H = 30.0$  cm. A rigid plastic sheet, which acted as a false bottom spanning the tank width, was then inserted with one end at the surface at the right end of the tank and the other end touching the bottom a distance  $L_s$  from the right wall.  $L_s$  ranged from 26.5 cm to 120.3 cm depending upon the length of the plastic sheet used. The resulting constant slope,  $s$ , ranged from 0.25 to 1.13. The precision fit of the sheet pressing against the tank sidewalls held it in place during the setup and execution of the experiment.

Experiments were performed with gravity currents released from either full- or partial-depth locks. In a full-depth lock-release experiment, a water-tight gate was inserted into a vertical track located a distance  $L_\ell = 28.4$  cm from the left wall of the tank. Thus, the lock spanned approximately 1/6 the tank length. Because a gravity current is expected to propagate at constant speed for at least six lock-lengths along a horizontal bottom,<sup>9</sup> any deceleration of the gravity current observed in the experiments was attributed to upslope propagation. Indeed, in four experiments conducted with the slope placed closer to the lock, the results were identical even when  $L - L_\ell - L_s$  was reduced by half.

After the gate was inserted, a predetermined mass of salt was mixed into the lock and the resulting lock-density,  $\rho_\ell$ , was measured using an Anton Paar DMA 4500 density meter, which had a precision of 0.0001 g/cm<sup>3</sup>. The lock density ranged from 1.0010 g/cm<sup>3</sup> to 1.0500 g/cm<sup>3</sup> whereas the ambient fresh water typically had a density of 0.9985 g/cm<sup>3</sup>.

The lock-fluid was dyed with a small amount of food colouring for the purposes of flow visualization. The majority of the experiments were run with moderately shallow values of  $s$ , and with relatively small values of  $g'$ . These experiments make up the data points with a deceleration of 1.5 cm/s<sup>2</sup> or less. The experiments conducted with larger values of  $s$  and  $g'$ , though less directly applicable to environmental flows, served to validate (5) for a broad range of these parameters.

Partial-depth lock-release experiments were also run using a similar procedure to the one described above. However, for these experiments the gate contained an aperture located just below the free surface which was covered with a sponge and initially sealed with electrical tape. Salt was mixed into the lock-fluid as in the full-depth lock-release experiments. The seal was then removed from the aperture and salty fluid was slowly siphoned out of the bottom of the lock. Replacing the extracted salt water, fresh ambient fluid flowed through the aperture into the top of the lock. The

sponge served to minimize mixing between the fresh and salt water layers. Siphoning continued until the salt water in the lock fell to its desired depth,  $D$ , measured to an accuracy of 1 cm (Figure 1). Partial-depth experiments were performed with  $D/H = 0.50$  and  $0.75$ . The corresponding Reynolds numbers calculated from  $Re = D\sqrt{g'D}/\nu$ , ranged between  $8.6 \times 10^3$  and  $1.3 \times 10^5$ . Experiments with smaller  $D/H$  were not performed in order to ensure that the Reynolds number remained sufficiently large so that viscous effects had a negligible impact upon the observed upslope deceleration.

For all of the experiments, a bank of fluorescent bulbs was placed behind the tank and translucent white sheets were placed in front of these to provide nearly uniform background illumination. Movies of the experiments were recorded by a Canon EOS Rebel T3i digital camera situated 3 m in front of the tank midway along its length and midway between the free surface and bottom. The field-of-view was set so that the entire tank length was included.

## B. Observations and analyses

At the beginning of each experiment, the gate was swiftly extracted. The dense lock-fluid collapsed into the ambient and travelled as a classical gravity current moving along the horizontal bottom of the tank at constant speed until reaching the slope. Thereafter, the current progressed up the slope in the  $x'$ -direction with  $x = x' = 0$  denoting the base of the slope (see Figure 1). During this deceleration, particularly for the shallow-slope experiments, a progressively larger portion of the fluid fell back down the slope while the ever-thinning gravity current front continued to propagate in the positive  $x'$  direction. The gravity current front eventually stopped and subsequently ran back down the slope.

Figure 2 shows the evolution of a gravity current in a typical full-depth lock-release experiment. Panels (a), (b), and (c) show snapshots of the experiment at times prior to the removal of the gate, during horizontal propagation upon first reaching the slope, and during upslope propagation, respectively. Figure 2(b) shows that the head height of the gravity current over the horizontal surface is approximately half the ambient depth, as predicted from Benjamin's<sup>6</sup> energy-conserving theory. Figure 2(c) shows that the shape of the gravity current thins as it propagates upslope. This evolution was common for all experiments.

To evaluate the position of the gravity current front, time-series were constructed from movies of the experiments. Horizontal time-series were generated by extracting horizontal slices from successive frames, the slice being located 1 cm above the bottom of the tank so as to avoid including in the image any fluid that had leaked from the lock prior to the gate extraction. The slices spanned a horizontal distance  $L - L_s$  from the left-end wall of the tank. Diagonal time-series were constructed from diagonal slices taken 0.5 cm above the sloping false-bottom. The slices in question began at the tank bottom, ran along the sloping line segment  $x' = x\sqrt{s^2 + 1}$ , and ended at the free surface. Results were plotted with the horizontal co-ordinate system having  $x < 0$  before the slope and  $x' > 0$  along the slope (Figures 2(d) and 2(e)). By convention, time was set so that the front reached the base of the slope (at  $x = x' = 0$ ) at time  $t = 0$ .

Using the horizontal and diagonal time-series from each experiment, data points were extracted and used to create graphs of time versus front position (insets in Figures 2(d) and 2(e)). The data points were obtained by visually identifying the interface between the dyed lock-fluid and the clear ambient. In cases for which the location of the interface was unclear, its position was estimated to be where the dye had an intensity approximately equal to the average dye intensity of the ambient and lock fluids.

The front speed,  $u_0$ , of the gravity current as it approached the slope was found from the slope of the least-squares best-fit line through the data points of  $x$  versus  $t$  for the nose position taken from the horizontal time-series image. For example, from the best-fit line through the data shown in Figure 2(d) (inset), it was found that  $u_0 = 3.74$  cm/s. The corresponding Froude number was 0.45 for this experiment.

The deceleration of the front was found from the least-squares best-fit quadratic that was fit to the data points corresponding to the current front in the diagonal time-series. Explicitly, the along slope deceleration,  $d_{x'}$ , was set to be twice the coefficient of the  $t^2$  term and the horizontal

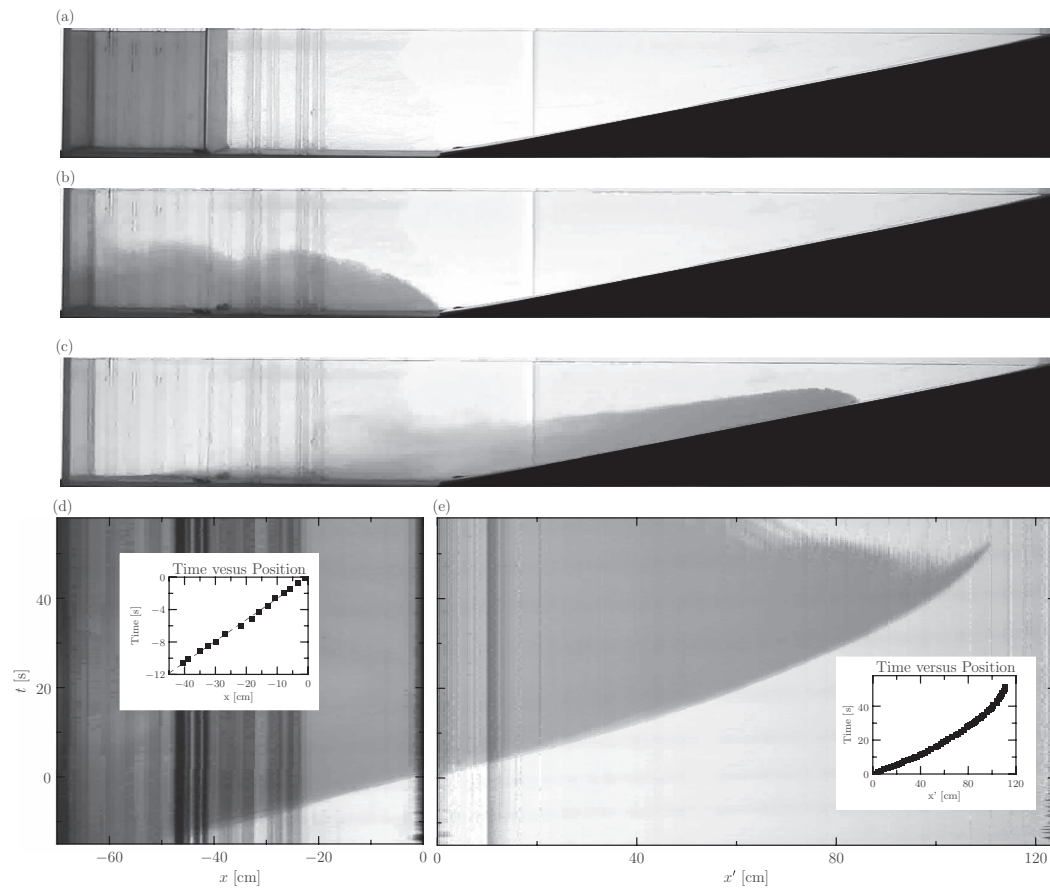


FIG. 2. Results of a full-depth lock-release experiment with  $D = H = 30.0$  cm,  $\rho_\ell = 1.001$  g/cm<sup>3</sup> and  $s = 0.25$ . Snapshots show the gravity current at times (a)  $t = -10$  s, (b)  $0$  s, and (c)  $30$  s with fields of view measuring  $197.5$  cm long  $\times$   $30.2$  cm tall. (d) Front position as a function of time,  $t$ , prior to encountering the slope shown as a horizontal time-series and a plot of the extracted data points with the dashed least-squares best-fit line (inset). (e) Front position as a function of time as the gravity current propagated upslope shown as a diagonal time-series and a plot of the extracted data points overlying the dashed least-squares best-fit quadratic curve (inset).

component of this deceleration was set to be  $d_x = d_{x'}/\sqrt{s^2 + 1}$ . For example, from the data shown in Figure 2(e) (inset) the along slope deceleration was found to be  $d_{x'} = 0.062$  cm/s<sup>2</sup> and the horizontal deceleration was found to be  $d_x = 0.060$  cm/s<sup>2</sup>.

The evolving shape of the gravity current head between the nose and the base of the slope was examined by comparing the profiles of gravity current height above the slope,  $h(x, t)$ , measured at five equally spaced times, where  $t_{\max}$  corresponds to the point where the front ceased moving upslope. For each value of  $t$ ,  $h(x, t)$  was measured at 20 horizontal positions,  $x$ , over the slope. The function was then rescaled first by dividing  $h$  by the gravity current height at the base of the slope,  $h_0(t)$ , and then by dividing  $x$  by the front position  $x_f(t)$ . These definitions of  $h$ ,  $h_0$ , and  $x_f$  are illustrated in Figure 3.

## IV. RESULTS

### A. Horizontal speed before the slope

Consistent with related experimental<sup>9,10</sup> and numerical studies<sup>25</sup> of bottom-propagating gravity currents on horizontal surfaces, the gravity current front attained a constant speed within 1 s after removal of the gate and it maintained that speed until reaching the base of the slope (e.g., see Figure 2(d)). For all experiments, the front speed,  $u_0$ , was measured and the corresponding Froude

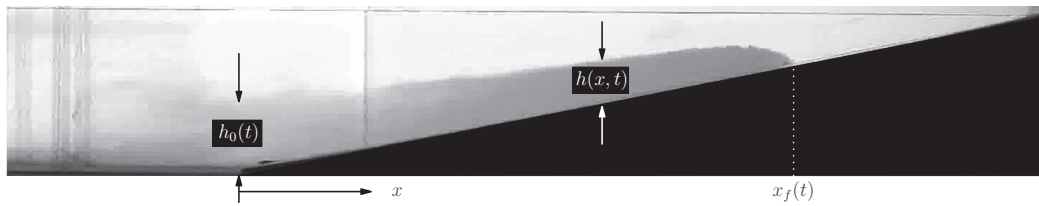


FIG. 3. Schematic indicating variables used to nondimensionalize the gravity current shape.

number,  $Fr_D$ , was calculated using (1). This was compared to existing theoretical and experimental values. The Froude numbers of the full-depth lock-release experiments had an average value of  $Fr_D = 0.45 \pm 0.02$ . This was slightly smaller than the value predicted by Benjamin<sup>6</sup> but was consistent with other experimental findings.<sup>7,10,11</sup> The Froude numbers for the  $D/H = 3/4$  and  $D/H = 1/2$  experiments had average values of  $Fr_D = 0.46 \pm 0.03$  and  $0.40 \pm 0.04$ , respectively. These results are also consistent, within error, with the measurements made by Shin *et al.*,<sup>10</sup> who found  $Fr_D = 0.48$  and  $0.44$ , respectively, and are consistent with the predictions given by (2) of  $Fr_D = 0.48$  and  $0.43$ , respectively. For both full- and partial-depth lock-release experiments, energy loss due to mixing is believed to be the reason that the experimental results are over-predicted by theory.

## B. Front deceleration along the slope

In all experiments, the gravity current front slowed down immediately upon reaching the slope. This immediate deceleration was most obvious in cases with larger values of  $s$  and  $g'$ . Furthermore, between first encountering the slope and finally coming to rest, the deceleration of the front was nearly uniform. As shown in Figure 4, the measured deceleration scales with  $g'$ ,  $s$ , and  $D/H$  in a way that is consistent with the theoretical prediction given by (5). No systematic deviation from this prediction was found with  $s$ . The dashed line of Figure 4 is the least-squares best-fit line of the entire data set and has a slope of  $0.112 \pm 0.002$  leading to the following empirical relationship for the rate

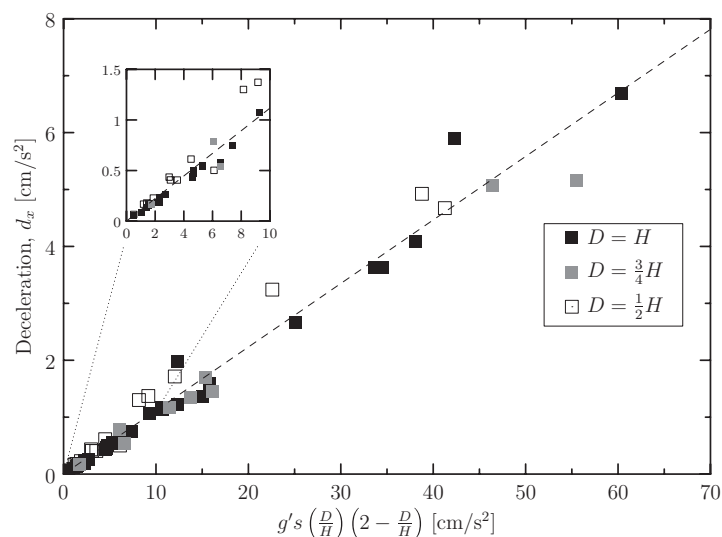


FIG. 4. Deceleration of the gravity current head found from a multitude of experiments that varied the slope,  $s$ , from 0.24 to 1.14 and the reduced gravity,  $g'$ , from  $2 \text{ g/cm}^3$  to  $73 \text{ g/cm}^3$ . The dotted line is a least-squares line of best-fit. The error of each data point is approximately equal to the size of the markers in the main figure.

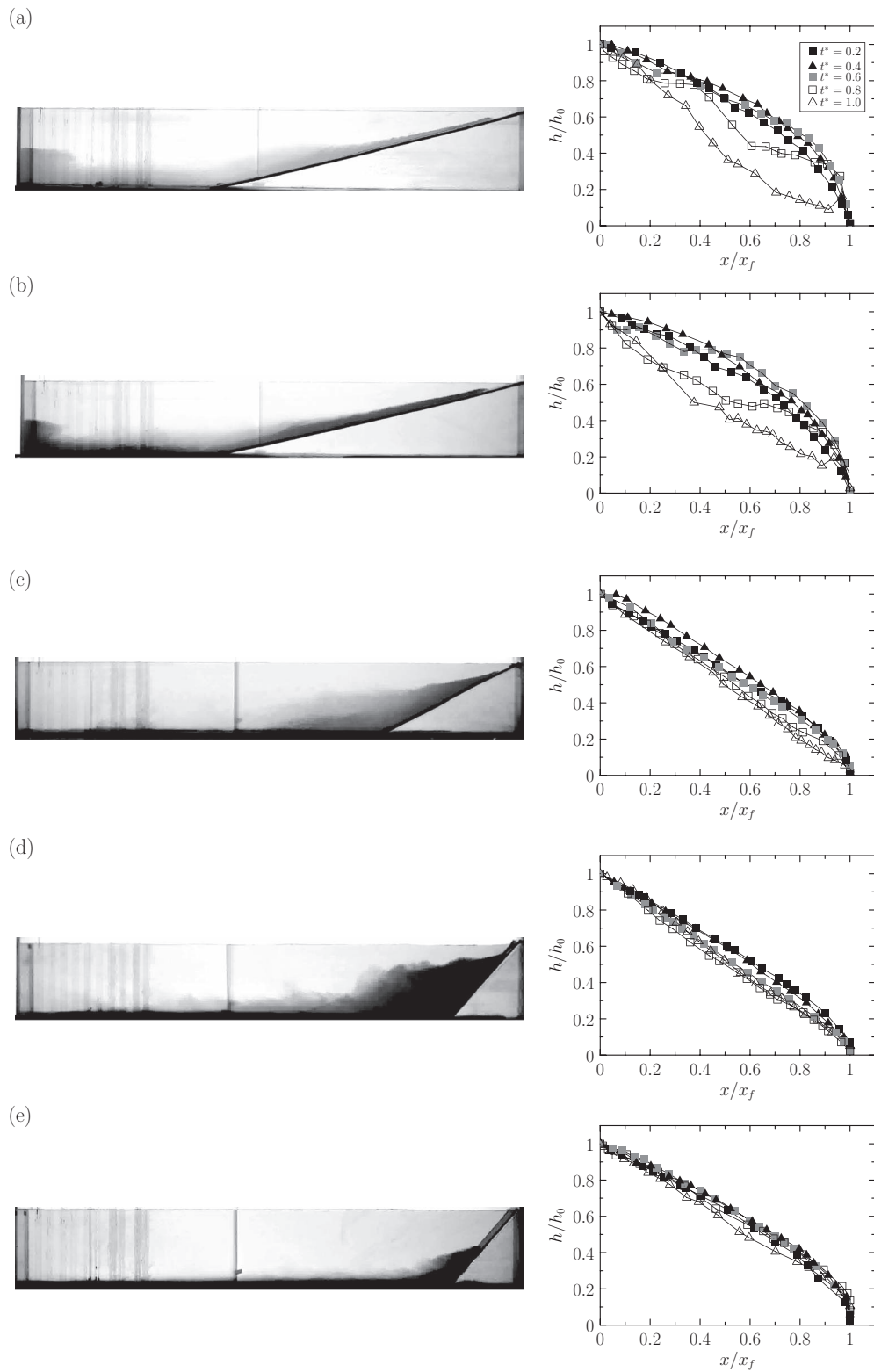


FIG. 5. Comparison of gravity current shapes in five different experiments with indicated  $D/H$ ,  $s$ , and  $g'$ . Snapshots show gravity currents at the instant the front has reached its maximum upslope elevation. Plots of nondimensional height vs nondimensional horizontal position (right) are given at five different times ( $t^* = 0.2, 0.4, 0.6, 0.8, 1.0$ ) as indicated by the legend in the top-right plot. (a)  $D/H = 1$ ,  $s = 0.25$ ,  $g' = 22 \text{ g/cm}^2$ ; (b)  $D/H = 1$ ,  $s = 0.25$ ,  $g' = 44 \text{ g/cm}^2$ ; (c)  $D/H = 1$ ,  $s = 0.58$ ,  $g' = 44 \text{ g/cm}^2$ ; (d)  $D/H = 1$ ,  $s = 1.1$ ,  $g' = 52 \text{ g/cm}^2$ ; and (e)  $D/H = \frac{1}{2}$ ,  $s = 1.1$ ,  $g' = 44 \text{ g/cm}^2$ .



of deceleration of the gravity current front:

$$d_x = (0.112 \pm 0.002)g's \left(\frac{D}{H}\right) \left(2 - \frac{D}{H}\right). \quad (8)$$

The numerical prefactor shows robust agreement with the predicted value of  $1/8$ , which is remarkable considering the relative simplicity of the theory outlined in Sec. II.

A comparison of the experimental results and the prediction of (7) shows significantly greater scatter. In particular, the deceleration predicted by (7) is double that given by (5) in the case  $D = H/2$ . Therefore, the open squares in Fig. 4 would lie far to the right of the corresponding dashed line if (7) was used in place of (5).

### C. Shape analysis

Figure 5 depicts the evolution of the gravity current shape during upslope propagation for five different experiments. The snapshot image on the left side of each panel shows the gravity current at its maximum upslope position. In each case, it can be seen that the gravity current fluid attains a height below  $H$  and slightly different than  $D$ , its initial height inside the lock. From many experiments, it was found that the gravity current fronts reached average heights of  $z_{\max} = 0.86D$  ( $0.86H$ ),  $0.99D$  ( $0.74H$ ), and  $1.15D$  ( $0.58H$ ) for cases with  $D/H = 1$ ,  $0.75$ , and  $0.5$ , respectively. In light of the prediction following from (5) and (6) that  $z_{\max} = H$ , one might expect larger measured values of  $z_{\max}$ . However, the prediction neglects along-slope gravitational deceleration and viscosity, both of which exert a nontrivial influence over and above that associated with the ambient return flow as the front approaches its maximum height. The measured deceleration nonetheless agrees well with (5) because we apply a least-squares quadratic best fit to plots of the front position vs. time; this method is statistically weighted toward determining the deceleration over the relatively long times when viscosity remains comparatively unimportant.

The gravity current shape is much thinner and more elongated on the shallower slopes as compared to the thicker gravity currents observed on steep slopes. The plots shown on the right side of each panel in Figure 5 depict the nondimensional gravity current height versus the nondimensional horizontal position at various nondimensional times,  $t^*$ , where  $t^* = t/t_{\max}$ . The overlap of the rescaled gravity current shapes indicates that the gravity current maintains a nearly self-similar shape during much of its upslope propagation. Specifically, in all cases shown, the decrease of the nondimensionalized head height was linear between the start of the slope and up to approximately 80% of the distance to the nose and up until  $t^* = 0.8$ . The self-similarity is most prominent when the slope is steep (Figures 5(c)–5(e)) in which case the deceleration time was brief and little fluid flowed downslope prior to the front reversing direction from upslope to downslope flow. Conversely, in experiments with a shallow slope (Figures 5(a) and 5(b)), the front took a longer time to decelerate, in which case a larger volume of dense fluid from behind the front reversed direction and flowed downslope before the front reached its maximum height. This downslope flow increased the value of  $h_0(t)$ , resulting in smaller values of  $h/h_0$  and a deviation from the self-similar shape evident at earlier times or for larger values of  $s$ .

## V. DISCUSSION AND CONCLUSIONS

An examination of Boussinesq, high Reynolds number gravity currents propagating up-slope was conducted through rectilinear full- and partial-depth lock-release experiments with various slopes and various values of reduced gravity. The dynamics of interest here are qualitatively different from those associated with downslope flow; a gravity current front propagating upslope must decelerate and ultimately reverse direction, whereas a front moving downstream may reach a constant velocity when gravity exactly balances the influence of entrainment and basal friction.

A WKB-like theory was developed as an extension of the existing theory<sup>6,10,24</sup> to determine a heuristic prediction for the along slope deceleration of the gravity current flow. Consistent with this theory, it was found that the gravity current front propagated at a constant velocity along the horizontal portion of the tank and experienced near constant deceleration as soon as it began propagating

upslope. More quantitatively, the relationship for the horizontal component of deceleration was best estimated by (5):  $d_x = g's(D/H)(2 - D/H)/8$ . The coefficient of  $1/8$  agrees well with the experimentally measured value of  $0.112 \pm 0.002$ . By comparison, Sutherland *et al.*<sup>24</sup> found that a full-depth lock-release surface gravity current propagating over a bottom slope decelerated as  $d_x = 0.31g's$ . The magnitude of deceleration was larger in these experiments because the deceleration did not start until the nose was approximately halfway over the slope and, therefore, the front stopped over a shorter distance.

The shape analysis revealed that the gravity current head steadily reduced in height as it propagated upslope. For steep slopes (Figures 5(c)–5(e)) its shape, being scaled by the gravity current height at the base of the slope and the along-slope length, showed strong self-similarity. For shallow slopes, this self-similarity was less robust.

The range of parameters explored here provides a starting point for understanding gravity currents propagating in complex environments occurring in industry and in the environment. Ongoing work is examining gravity currents propagating in V-shaped canyons (C. S. Jones, personal communication). Future work will explore gravity currents propagating upslope in ambient fluid of nonuniform density to provide a model that more realistically captures coastal sea breezes interacting with atmospheric inversions.

## ACKNOWLEDGMENTS

These experiments were inspired in part by conversations with Stuart Dalziel and the (unpublished) Ph.D. research of Matthew Brown performed in the mid-1990s at the University of Cambridge. This work was supported in part by funding from the Natural Sciences and Engineering Research Council through the Discovery Grant and Research Tools and Instruments programs.

- <sup>1</sup> J. E. Simpson, "Gravity currents in the laboratory, atmosphere, and ocean," *Annu. Rev. Fluid Mech.* **14**, 213–234 (1982).
- <sup>2</sup> J. E. Simpson, *Gravity Currents*, 2nd ed. (Cambridge University Press, Cambridge, England, 1997).
- <sup>3</sup> J. E. Simpson, *Sea Breeze and Local Winds* (Cambridge University Press, Cambridge, England, 1994).
- <sup>4</sup> G. H. Keulegan, "An experimental study of the motion of saline water from locks into fresh water channels," Technical Report No. 5168, Nat. Bur. Stand. Rept., 1957.
- <sup>5</sup> G. H. Keulegan, "The motion of saline fronts in still water," Technical Report No. 5831, Nat. Bur. Stand. Rept., 1958.
- <sup>6</sup> T. B. Benjamin, "Gravity currents and related phenomena," *J. Fluid Mech.* **31**, 209–248 (1968).
- <sup>7</sup> J. E. Simpson, "Effects of lower boundary on the head of a gravity current," *J. Fluid Mech.* **53**, 759–768 (1972).
- <sup>8</sup> H. E. Huppert and J. E. Simpson, "The slumping of gravity currents," *J. Fluid Mech.* **99**, 785–799 (1980).
- <sup>9</sup> J. W. Rottman and J. E. Simpson, "Gravity currents produced by instantaneous releases of a heavy fluid in a rectangular channel," *J. Fluid Mech.* **135**, 95–110 (1983).
- <sup>10</sup> J. O. Shin, S. B. Dalziel, and P. F. Linden, "Gravity currents produced by lock exchange," *J. Fluid Mech.* **521**, 1–34 (2004).
- <sup>11</sup> H. E. Huppert, "The propagation of two-dimensional and axisymmetric viscous gravity currents over a rigid horizontal surface," *J. Fluid Mech.* **121**, 43–58 (1982).
- <sup>12</sup> Z. Borden and E. Meiburg, "Circulation based models for Boussinesq gravity currents," *Phys. Fluids* **25**, 101301 (2013).
- <sup>13</sup> G. F. Lane-Serff, L. M. Beal, and T. D. Hadfield, "Gravity current flow over obstacles," *J. Fluid Mech.* **292**, 39–53 (1995).
- <sup>14</sup> M. Ungarish, *An Introduction to Gravity Currents and Intrusions* (CRC Press, Boca Raton, FL, USA, 2009).
- <sup>15</sup> R. E. Britter and P. F. Linden, "The motion of the front of a gravity current travelling down an incline," *J. Fluid Mech.* **99**, 531–542 (1980).
- <sup>16</sup> A. Dai, "Experiments on gravity currents propagating on different bottom slopes," *J. Fluid Mech.* **731**, 117–141 (2013).
- <sup>17</sup> A. Dai, "Non-Boussinesq gravity currents propagating on different bottom slopes," *J. Fluid Mech.* **741**, 658–680 (2014).
- <sup>18</sup> E. Meiburg and B. Kneller, "Turbidity currents and their deposits," *Annu. Rev. Fluid Mech.* **42**, 135–156 (2010).
- <sup>19</sup> C. Cenedese and C. Adduce, "Mixing in a density driven current flowing down a slope in a rotating fluid," *J. Fluid Mech.* **604**, 369–388 (2008).
- <sup>20</sup> C. Adduce, G. Sciortino, and S. Proietti, "Gravity currents produced by lock exchanges: Experiments and simulations with a two-layer shallow-water model with entrainment," *J. Hydraul. Eng.* **138**, 111–121 (2012).
- <sup>21</sup> R. J. Lowe, P. F. Linden, and J. W. Rottman, "A laboratory study of the velocity structure in an intrusive gravity current," *J. Fluid Mech.* **456**, 33–48 (2002).
- <sup>22</sup> Note that "WKB" refers to Wentzel, Kramers, and Brillouin who developed a method to find approximate solutions of linear differential equations with coefficients that vary slowly in space and time.
- <sup>23</sup> C. Härtel, E. Meiburg, and F. Necker, "Analysis and direct numerical simulation of the flow at a gravity-current head. Part 1. Flow topology and front speed for slip and no-slip boundaries," *J. Fluid Mech.* **418**, 189–212 (2000).
- <sup>24</sup> B. R. Sutherland, D. Polet, and M. Campbell, "Gravity currents shoaling on a slope," *Phys. Fluids* **25**, 086604 (2013).
- <sup>25</sup> C. Härtel, E. Meiburg, and F. Necker, "Vorticity dynamics during the start-up phase of gravity currents," *Il Nuovo Cimento* **22**, 823–833 (1999).